Low-bandgap conjugated polymer for high efficient photovoltaic applications†

Yi-Chun Chen, Chao-Ying Yu, Yu-Ling Fan, Ling-I Hung, Chih-Ping Chen* and Ching Ting*

Received 23rd April 2010, Accepted 9th July 2010
DOI: 10.1039/c0cc01087a

We investigate the morphological and performance of organic photovoltaics based on blended films of alternating poly-(thiophene–phenylene–thiophene) and [6,6]-phenyl-C_{71}-butyric acid methyl ester ($PC_{71}BM$). The resulting fine-scale phase separation leads to enhanced performance and the highest power efficiency (6.4% under AM 1.5G (100 mW cm^{-2})) when we use solvent annealing process.

The research field of organic photovoltaics (OPVs) is flourishing due to its promising application advantages such as flexibility, light weight, potential high efficiency and solution-processability.[1–5] For OPVs with low band gap (LBG) materials,[6–10] processing into large area devices[11–13] with long-term stability[14] has been widely investigated. With the innovation of materials engineering, the power conversion efficiency (PCE) of OPVs has been improved up to 7.9% using new active layer materials.[15,16] This encouraging progress advances such technology towards commercial application.[17] To push the PCE of OPVs towards predicted theoretical limits,[18] simultaneously achieving a high short circuit current (J_{sc}) and a high open circuit voltage (V_{oc}) is critical. Theoretically, the extended absorption of sunlight at longer wavelengths directly reflects the value of J_{sc}. Nevertheless, film characteristic and optoelectronic properties like absorption coefficient will change this value.[7] The V_{oc} of OPVs is dominated by the difference between the LUMO of the acceptor (fullerene) and the HOMO of the donor (polymer). Furthermore, the LUMO difference between conjugated polymer and fullerene should be greater than 0.3 eV to ensure efficient exciton dissociation.[1–3] Because these parameters are often inter-correlated, it is a great challenge to design and synthesize a polymer to meet all the challenging points required for high efficient OPV application.

Previous studies on thiophene/phenylene/thiophene (TPT)-based derivatives have shown efficient OPV characteristics.[6,7] These polymers exhibit better harvesting of solar flux with deeper HOMOs that give impressively larger V_{oc} (>0.8 V) and possess OPV performance up to 4.3%. Those previous polymers were synthesized from di-bromine TPT monomer and the structures were limited to a random feature. Through a rational molecular engineering approach, we describe an alternating TPT based conjugated polymer for high efficiency OPV, which exhibits a PCE of 6.4% under the AM 1.5G (100 mW cm^{-2}) condition. An alternating polymer (***a*-PTPTBT**) that consists of TPT as the electron-donating unit and 2,1,3-benzothiadiazole (BT) as the electron-accepting moiety was synthesized by Pd(0)-catalyzed Stille coupling polymerization in chlorobenzene under microwave heating conditions (Scheme 1).

The newly synthesized di-tin TPT precursor enables the synthesis of various TPT-based polymers with well-defined alternating structures. The structures of earlier synthesized random TPT polymers are not controllable and are likely to feature a random distribution of TPT and acceptor-rich moieties. Details of the synthesis and characterization are included in the ESI.† As a result of GPC, the ***a*-PTPTBT** shows a M_w of 60.9 kg mol^{-1} with a PDI of 2.51. The ***a*-PTPTBT** possesses good thermal stability [5% weight-loss temperature (Td) > 450 °C] as indicated by thermogravimetric analysis (TGA). When investigating the thermal behavior of the polymer using differential scanning calorimetry (DSC), we observed no clear thermal transitions in the temperature range from 40 to 300 °C. Fig. 1 displays the UV-vis absorption features of the polymer film in the solid state. The polymer bandgap is 1.75 eV with an absorption coefficient of 1.60 × 10^5 cm^{-1} for the polymer film at λ_{max} (= *ca.* 570 nm). Two characteristic bands in the absorption spectrum were found in which the shorter wavelength absorbance originated from the π–π* transition of the TPT units, while the lower energy band was attributed to the intramolecular charge transfer (ICT) between the electron-rich and the BT segments. The HOMO and LUMO energy levels of ***a*-PTPTBT** are determined from cyclic voltammograms (CVs) to be −5.36 and −3.52 eV, respectively. According to a previous report, the LUMO and HOMO of PCBM are −3.94 and −5.93 eV, respectively.[7] The LUMO offset of the polymer and PCBM is large enough for energetically efficient charge transfer and therefore allows devices to exhibit higher current output. Furthermore, the V_{oc} can be improved by the relatively deeper HOMO energy level of the polymer.

Table 1 and Fig. 2(a) display the output characteristics of the devices prepared under various fabrication conditions. The ***a*-PTPTBT**/$PC_{71}BM$ cell exhibited averaged AM 1.5G (100 mW cm^{-2}) PCEs of *ca.* 5.4%. In comparison with the

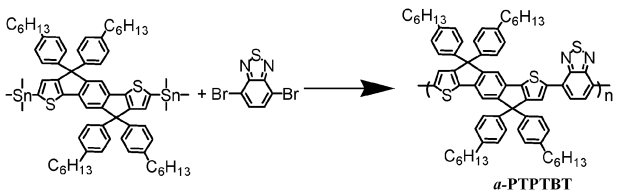

Scheme 1 The synthetic route to ***a*-PTPTBT**.

Materials and Chemical Laboratories, Industrial Technology Research Institute, 195, Sec. 4, Chung Hsing Road, Chutung, Hsinchu, 310, Taiwan. E-mail: chihping_chen@itri.org.tw, cting@itri.org.tw; Fax: 886-35-827694; Tel: 886-35-93588

† Electronic supplementary information (ESI) available: A description of experimental procedures including structural characterization. See DOI: 10.1039/c0cc01087a

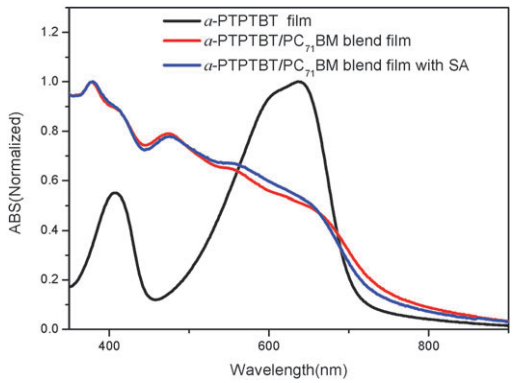

Fig. 1 UV-vis absorption spectra of the ***a*-PTPTBT** and the blend films.

devices based on similar random **PTPTBT**,[6,7] the PCE increases by *ca.* 30%, while J_{sc} and V_{oc} show a slight improvement. This is primarily due to the fill factor (FF). It is known that the hole mobility of polymer should be higher for effective carrier transport, which directly affects the FF of device. To evaluate the contribution of polymer mobility, we employed hole-only devices to characterize the hole mobility of blend films.[19,20] We calculated the field-independent mobility of the ***a*-PTPTBT** and random **PTPTBT** derived devices to be 2.2×10^{-9} m^2/Vs and 1.9×10^{-10} m^2/Vs, respectively. As expected, the mobility of the alternating TPT derivate is one order of magnitude higher than that for random derivates, which enables better carrier transport within active layer and produces greater FF. In an attempt to further improve device performance, we utilized strategies based on thermal annealing, slow drying, and solvent vapor annealing (SA).[21–23] We found that the PCE of devices can be significantly increased *via* the SA process. The devices were placed inside a Petri dish for annealing with saturated DCB vapor for 10–30 min. The most efficient SA-fabricated device exhibited a PCE of 6.4% under AM 1.5G irradiation (100 mW cm^{-2}), with J_{sc}, V_{oc}, and FF values of 11.2 mA cm^{-2}, 0.85 V, and 0.67, respectively. In comparison with the normal device, the FF of SA-fabricated device underwent a significant increase of *ca.* 12%, whereas the J_{sc} increased only slightly. The PCEs of these SA-fabricated devices were reproducible, with a variation of only 10% exhibited among five individual PSC devices. The performance of this OPV device is among the highest ever reported. To confirm the accuracy of the measurements, the external quantum efficiency (EQE) of the devices was measured. Fig. 2(b) displays the EQE spectra of the devices fabricated with ***a*-PTPTBT**:$PC_{71}BM$ blend films. The SA-fabricated device reveals a significant contribution of EQE in the wavelength between 350 nm and 750 nm and is consistent with UV-vis spectrum of blend film (Fig. 1) with the maximum EQE being approximately 63% at 470 nm. Convolution of the spectral response with the photon flux AM 1.5G spectrum gives an estimate for the J_{sc} under irradiation to be 10.6 mA cm^{-2}. Due to the mismatch between EQE and photon flux AM 1.5G, there is an approximately 5% mismatch between convolution and solar simulator data. The EQE of normal device is close to SA device and is consistent with the J_{sc} values obtained from these two methods. Note that the shape of the

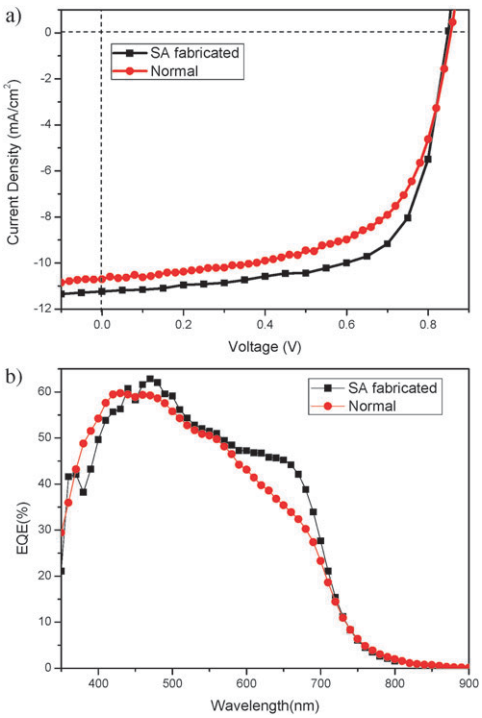

Fig. 2 (a) Current density-potential characteristics of ***a*-PTPTBT**/$PC_{71}BM$ devices under illumination with AM 1.5G solar simulated light (100 mW cm^{-2}). (b) The EQE spectra of devices fabricated with ***a*-PTPTBT** /$PC_{71}BM$.

EQE curves is different after SA process. The relative enhancement of EQE from 600 nm to 700 nm is likely due to different spatial distribution of ***a*-PTPTBT** and PCBM.[24] We also determined the SCLC hole and electron mobilities of the respective devices. The result shows that hole mobility of SA-fabricated device is 2.4×10^{-9} m^2/Vs and reveals no significant change between the normal and SA devices. The determined electron mobilities of SA and normal devices are 2.6×10^{-8} and 1.6×10^{-8} m^2/Vs, respectively. A small increase of the electron mobility from 1.6×10^{-8} to 2.6×10^{-8} m^2/Vs is observed after the SA process. The preliminary result indicates that the carrier mobilities in both devices are balanced and within the reasonable range.

Besides the mobility, we suspect the differing morphology also contributes to variations in device performance. To confirm this correlation, we recorded TEM images of respective blend films (Fig. 3). Because the electron scattering density of PCBM is higher than that of the conjugated polymer, the ***a*-PTPTBT** domains appear as bright regions whereas the dark regions can be attributed to PCBM domains.

Table 1 OPV parameters of devices based on **PTPTBT** polymers

	J_{sc}/mA cm^{-2}	V_{oc}/V	FF (%)	PCE (%) Best	PCE (%) Ave
***a*-PTPTBT**[a]	8.1	0.87	64.9	4.56	4.3
***a*-PTPTBT**[b]	10.7	0.86	60.4	5.56	5.4
PTPTBT[b]	10.1	0.80	53.0	4.30	4.0
***a*-PTPTBT-SA**[b]	11.2	0.85	67.2	6.41	6.1

[a] Using $PC_{61}BM$ (Purchased from Nano-C) as acceptors. [b] Using $PC_{71}BM$ (Purchased from Solenne) as acceptors.

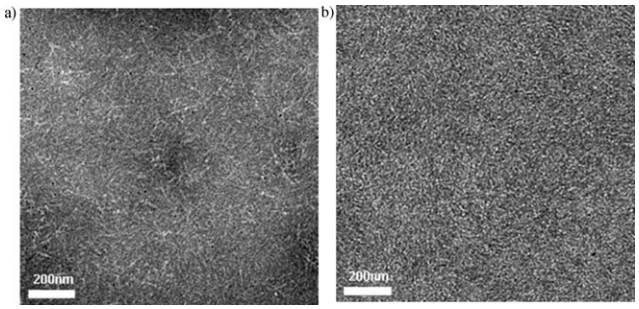

Fig. 3 TEM images of ***a*-PTPTBT** : $PC_{71}BM$ films before (a) and after solvent annealing (b). (The scale bar is 200 nm).

The normal blend film [Fig. 3(a)] exhibits morphology with separated ***a*-PTPTBT** domains and PCBM domains; the fibrillar features of the polymer are clearly seen. In contrast, the SA film [Fig. 3(b)] reveals that it consists of well-defined blends of PCBM domains (having grain size *ca.* 20–30 nm) surrounded by ***a*-PTPTBT** domains. The SA process optimizes the miscibility of the polymer with PCBM, leading to better phase separation between polymer chains and PCBM molecules formation of interpenetrating networks (IPNs). Furthermore, the morphology of the SA blend film is much more uniform and there is no large phase separation. As a result, the SA blend system has preferred IPN morphology to ensure the efficient charge separation and transport required in higher cell performance. For the widely investigated P3HT system, in which the fibril-like structure typically, correlates to the high crystallinity as well as the performance.[25] The solvent vapor treatment for P3HT system resulted in fine-tuned of nanoscale morphology and the enhancement of the carrier mobility.[26–28] Unlike P3HT system, our observation for ***a*-PTPTBT** system is different after SA. To our knowledge, the correlation between morphology, performance and carrier mobility is not clear for new designed polymers. For instance, the use of additive (alkane-dithiols) has resulted in a significant improvement of performance for a device based on poly[2,6-(4,4-bis(2-ethylhexyl)-4*H*-cyclopenta[2,1-b;3,4-b]dithiophene)-alt-4,7-(2,1,3-benzothiadiazole)] (PCPDTBT).[9,29] The well-organized morphology of the PCPDTBT device was observed in the presence of an additive. Nevertheless, the hole mobility of the device showed no increase either from space charge limited current (SCLC) model[29] or FETs[9] result. We speculate that the effect stems from the spatial distribution of donor and acceptor domains rather than intrinsic differences in carrier mobilities.[9,29] Further study is underway to verify the difference between these polymers.

To conclude, we have demonstrated high performance OPV devices by using alternating TPT copolymer. The alternating TPT polymer shows higher SCLC hole mobility than its random derivative. We used SA treatment to achieve optimized bulk hetero-junction morphology. The devices with PCEs up to 6.4% and high fill factor of over 67% were obtained. Further investigations are currently underway to fine-tune the material's energy bandgap. A further improvement in PCE can be expected if the J_{sc} of the device can be further enhanced.

We thank the Ministry of Economic Affairs, Taiwan, for financial support.

Notes and references

1 B. C. Thompson and J. M. J. Fréchet, *Angew. Chem., Int. Ed.*, 2008, **47**, 58.
2 P. Heremans, D. Cheyns and B. Rand, *Acc. Chem. Res.*, 2009, **42**, 1740.
3 M. Helgesen, R. Søndergaard and F. C. Krebs, *J. Mater. Chem.*, 2010, **20**, 36.
4 G. Dennler, M. C. Scharber and C. J. Brabec, *Adv. Mater.*, 2009, **21**, 1323.
5 J. Lu, F. Liang, N. Drolet, J. Ding, Y. Tao and R. Movileanu, *Chem. Commun.*, 2008, 5315.
6 C.-P. Chen, S.-H. Chan, T.-C. Chao, C. Ting and B.-T. Ko, *J. Am. Chem. Soc.*, 2008, **130**, 12828.
7 C.-Y. Yu, C.-P. Chen, S.-H. Chan, G.-W. Hwang and C. Ting, *Chem. Mater.*, 2009, **21**, 3262.
8 S. H. Park, A. Roy1, S. Beaupré, S. Cho, N. Coates, J. S. Moon, D. Moses, M. Leclerc, K. Lee and A. J. Heeger, *Nat. Photonics*, 2009, **3**, 297.
9 J. Peet, J. Y. Kim, N. E. Coates, W. L. Ma, D. Moses, A. J. Heeger and G. C. Bazan, *Nat. Mater.*, 2007, **6**, 497.
10 M. Wienk, M. Turbiez, J. Gilot and R. A. J. Janssen, *Adv. Mater.*, 2008, **20**, 2556.
11 F. C. Krebs, S. A. Gevorgyan and J. Alstrup, *J. Mater. Chem.*, 2009, **19**, 5442.
12 F. C. Krebs, *Sol. Energy Mater. Sol. Cells*, 2009, **93**, 465.
13 L. Blankenburg, K. Schultheis, H. Schache, S. Sensfuss and M. Schrödner, *Sol. Energy Mater. Sol. Cells*, 2009, **93**, 476.
14 M. Jørgensen, K. Norrman and F. C. Krebs, *Sol. Energy Mater. Sol. Cells*, 2008, **92**, 686.
15 H. Y. Chen, J. Hou, S. Zhang, Y. Liang, G. Yang, Y. Yang, L. Yu, Y. Wu and G. Li, *Nat. Photonics*, 2009, **3**, 649.
16 Y. Liang, Y. Wu, D. Feng, S.-T. Tsai, H.-J. Son, G. Li and L. Yu, *J. Am. Chem. Soc.*, 2009, **131**, 56.
17 F. C. Krebs, T. D. Nielsen, J. Fyenbo, M. Wadstrøm and M. S. Pedersen, *Energy Environ. Sci.*, 2010, **3**, 512.
18 M. C. Scharber, D. Mühlbacher, M. Koppe, P. Denk, C. Waldauf, A. J. Heeger and C. J. Brabec, *Adv. Mater.*, 2006, **18**, 789.
19 O. G. Reid, K. Munechika and D. S. Ginger, *Nano Lett.*, 2008, **8**, 1602.
20 C. Melzer, E. J. Koop, V. D. Mihailetchi and P. W. M. Blom, *Adv. Funct. Mater.*, 2004, **14**, 865.
21 G. Li, V. Shrotriya, J. Huang, Y. Yao, T. Moriarty, K. Emery and Y. Yang, *Nat. Mater.*, 2005, **4**, 864.
22 W. L. Ma, C. Y. Yang, X. Gong, K. Lee and A. J. Heeger, *Adv. Funct. Mater.*, 2005, **15**, 1617.
23 J. K. Lee, W. L. Ma, C. J. Brabec, J. Yuen, J. S. Moon, J. Y. Kim, K. Lee, G. C. Bazan and A. J. Heeger, *J. Am. Chem. Soc.*, 2008, **130**, 3619.
24 H. Y. Chen, H. Yang, G. Yang, S. Sista, R. Zadoyan, G. Li and Y. Yang, *J. Phys. Chem. C*, 2009, **113**, 7946.
25 C. W. Chu, H. Yang, W. J. Hou, J. Huang, G. Li and Y. Yang, *Appl. Phys. Lett.*, 2008, **92**, 103306.
26 Y. Yao, J. Hou, Z. Xu, G. Li and Y. Yang, *Adv. Funct. Mater.*, 2008, **18**, 1783.
27 G. Li, Y. Yao, V. Shrotriya and Y. Yang, *Adv. Funct. Mater.*, 2007, **17**, 1636.
28 L. M. Chen, Z. R. Hong, G. Li and Y. Yang, *Adv. Mater.*, 2009, **21**, 1434.
29 M. Dante, A. Garcia and T.-Q. Nguyen, *J. Phys. Chem. C*, 2009, **113**, 1596.